ARTICLE

# FDG-PET patterns associated with underlying pathology in corticobasal syndrome

Matteo Pardini, MD, PhD, Edward D. Huey, MD, PhD, Salvatore Spina, MD, PhD, William C. Kreisl, MD, Silvia Morbelli, MD, PhD, Eric M. Wassermann, MD, Flavio Nobili, MD, Bernardino Ghetti, MD,* and Jordan Grafman, PhD*

**Correspondence**
Dr. Pardini
matteo.pardini@unige.it

*Neurology*® 2019;92:e1121-e1135. doi:10.1212/WNL.0000000000007038

## Abstract

### Objective

To evaluate brain $^{18}$Fluorodeoxyglucose PET (FDG-PET) differences among patients with a clinical diagnosis of corticobasal syndrome (CBS) and distinct underling primary pathologies.

### Methods

We studied 29 patients with a diagnosis of CBS who underwent FDG-PET scan and post-mortem neuropathologic examination. Patients were divided into subgroups on the basis of primary pathologic diagnosis: CBS-corticobasal degeneration (CBS-CBD) (14 patients), CBS-Alzheimer disease (CBS-AD) (10 patients), and CBS–progressive supranuclear palsy (CBS-PSP) (5 patients). Thirteen age-matched healthy patients who underwent FDG-PET were the control group (HC). FDG-PET scans were compared between the subgroups and the HC using SPM-12, with a threshold of $p_{FWE} < 0.05$.

### Results

There were no differences in Mattis Dementia Rating Scale or finger tapping scores between CBS groups. Compared to HC, the patients with CBS presented significant hypometabolism in frontoparietal regions, including the perirolandic area, basal ganglia, and thalamus of the clinically more affected hemisphere. Patients with CBS-CBD showed a similar pattern with a more marked, bilateral involvement of the basal ganglia. Patients with CBS-AD presented with posterior, asymmetric hypometabolism, including the lateral parietal and temporal lobes and the posterior cingulate. Finally, patients with CBS-PSP disclosed a more anterior hypometabolic pattern, including the medial frontal regions and the anterior cingulate. A conjunction analysis revealed that the primary motor cortex was the only common area of hypometabolism in all groups, irrespective of pathologic diagnosis.

### Discussion and conclusions

In patients with CBS, different underling pathologies are associated with different patterns of hypometabolism. Our data suggest that FDG-PET scans could help in the etiologic diagnosis of CBS.

*These authors contributed equally to this work.

From the Departments of Neuroscience, Rehabilitation, Ophthalmology, Genetics, and Maternal and Child Health (M.P., F.N.) and Health Sciences (S.M.), University of Genoa; IRCCS Ospedale Policlinico San Martino (M.P., S.M., F.N.), Genoa, Italy; Cognitive Neuroscience Division, Department of Neurology (E.D.H.), Gertrude H. Sergievsky Center, New York; Taub Institute for Research on Alzheimer's Disease and the Aging Brain (E.D.H., W.C.K.), Columbia University Medical Center, New York, NY; Department of Neurology (S.S.), UCSF Memory and Aging Center, UCSF, San Francisco, CA; Department of Pathology and Laboratory Medicine (S.S., B.G.), Indiana University School of Medicine, Indianapolis; Nuclear Medicine Unit (S.M.), IRCCS AOU San Martino, IST, Genoa, Italy; Behavioral Neurology Unit (E.M.W.), National Institute of Neurological Disorders and Stroke, NIH, Bethesda, MD; Psychiatry and Behavioral Sciences & Cognitive Neurology/Alzheimer's Disease Research Center (J.G.), Feinberg School of Medicine and Department of Psychology, Northwestern University; and Brain Injury Research, Cognitive Neuroscience Lab, Think and Speak Lab (J.G.), Shirley Ryan AbilityLab, Chicago, IL.

Go to Neurology.org/N for full disclosures. Funding information and disclosures deemed relevant by the authors, if any, are provided at the end of the article.

## Glossary

**AD** = Alzheimer disease; **ALS** = amyotrophic lateral sclerosis; **CBD** = corticobasal degeneration; **CBS** = corticobasal syndrome; **FDG** = $^{18}$Fluorodeoxyglucose; **FWE** = family-wise error; **HC** = healthy control; **HIPAA** = Health Insurance Portability and Accountability Act; **MDRS-2** = Mattis Dementia Rating Scale–2; **NINDS** = National Institute of Neurological Disorders and Stroke; **PC** = precuneus; **PCC** = posterior cingulate cortex; **PSP** = progressive supranuclear palsy; **ROI** = region of interest; **SPM** = statistical parametric mapping; **TOLA** = Test of Oral and Limb Apraxia; **WAIS-III** = Wechsler Adult Intelligence Scale III.

Corticobasal syndrome (CBS) is a disorder characterized by asymmetric akinetic-rigid syndrome, higher order sensory deficits, and cognitive impairment,[1] and its diagnosis requires competencies in movement disorders and neurobehavioral assessments. The clinical diagnosis of CBS has been associated with different neuropathologic substrata, including corticobasal degeneration (CBS-CBD), Alzheimer disease (CBS-AD), and progressive supranuclear palsy (CBS-PSP), with CBD the most frequent pathologic diagnosis, followed by AD and PSP.[2,3] Clinical features are insufficient to identify the underlying pathologic substrate of CBS with certainty during life.[1] $^{18}$Fluorodeoxyglucose PET (FDG-PET)[4] has been used to aid in CBS diagnosis, commonly showing an asymmetric frontoparietal pattern of cortical metabolism in many,[5,6] but not all studies.[7] The application of FDG-PET to try to differentiate the underlying pathologic substrata of CBS in vivo, however, has not been extensively explored,[6,8] even if available evidence suggests that different pathologies might show distinctive patterns of brain metabolism in CBS.

Patients with CBS with a positive amyloid PET scan, for example, have been shown to present with a more posterior pattern of hypometabolism compared to those with normal amyloid PET findings.[9] Here, we decided to systematically evaluate the association of a specific neuropathologic diagnosis with patterns of brain hypometabolism in a cohort of patients with CBS who underwent FDG-PET and postmortem neuropathologic examination. Our aims were (1) to test the existence of specific patterns of hypometabolism that are predictive of a distinctive neuropathologic substrate of CBS focusing on CBS-AD, CBS-CBD, and CBS-PSP, and (2) to identify whether common clusters of brain hypometabolism could be detected in patients with CBS irrespectively of the neuropathologic substrata.

## Methods

### Participants

Twenty-nine patients with (1) a diagnosis of CBS, (2) available FDG-PET brain imaging, and (3) a postmortem neuropathologic diagnosis of CBD, AD, or PSP were included in the study. Patients were derived from a cohort of 98 patients with CBS who were enrolled at the National Institute of Neurological Disorders and Stroke (NINDS) from 2001 to 2009; 36 of those had a pathologic postmortem diagnosis, as previously described from the clinical point of view by our group.[10,11] The 69 patients with CBS not included did not fulfill the criteria above. Patients were recruited from across the United States via advertisement and had to have an established diagnosis of CBS before coming to our attention. Clinical documentation was reviewed and the diagnosis of CBS was confirmed by a behavioral neurologist with experience in movement disorders (E.M.W.) and a neuropsychologist (J.G.) via consensus following a 1-week evaluation. Initial motor impairments in all of the patients with CBS consisted of an asymmetric progressive rigid syndrome resistant to therapeutic doses of levodopa evaluated in the months preceding the referral and confirmed at the clinical examination at the NINDS, associated with evidence of cortical deficits (as described by Boeve et al.[12]; the frequency of each cortical deficit for this cohort has been previously reported by our group[10]). All patients underwent detailed clinical and neuropsychological examination and structural brain imaging (MRI in all but 4 patients who underwent CT scans). Presence of significant vascular disease at structural imaging represented an exclusion criterion for the study; available images were reviewed also at the time of the statistical analysis to confirm the lack of significant vascular pathology. All imaging studies were carried out at NINDS. Neuropathologic studies were carried out at the Indiana University School of Medicine by dementia neuropathology experts (B.G. and S.S.). For all patients, laterality of the motor symptoms was available on file. Motor impairment was assessed with finger tapping test. Overall cognitive impairment was assessed using the Mattis Dementia Rating Scale–2 (MDRS-2). The Test of Oral and Limb Apraxia (TOLA)[13] and the Wechsler Adult Intelligence Scale III (WAIS-III) vocabulary score were used to assess praxis and language deficits. No quantitative sensory test was available. Patients' demographics are described in table 1.

### Neuropathologic evaluation

Brains were cut along the midsagittal plane. The left hemibrain was fixed in 10% buffered formalin, whereas the right hemibrain was frozen for genetic and biochemical studies. Sections were obtained from the following regions: superior and middle frontal gyri, cingulate gyrus, superior and middle temporal gyri, amygdala, superior parietal lobule, calcarine cortex, basal ganglia at the level of the anterior commissure, thalamus at the level of the subthalamic nucleus, anterior and posterior hippocampus, cerebellar cortex, dentate nucleus, midbrain, pons, and medulla.[14] Tissue was processed for hematoxylin & eosin, thioflavin S, and tau (AT8), β-amyloid, α-synuclein, and pTDP43 immunohistochemistry according

**Table 1** Main demographic and clinical characteristics of patients with corticobasal syndrome (CBS)

| | | | Patients with CBS divided according to pathologic diagnosis | | |
|---|---|---|---|---|---|
| | HC (n = 13) | CBS (n = 29) | CBD (n = 14) | PSP (n = 5) | AD (n = 10) |
| **Age at onset, y** | — | 60.4 ± 7.8 | 63.2 ± 5.4 | 64.6 ± 6.0 | 54.5 ± 5.8 |
| **Age at evaluation, y** | 61.5 ± 6.2 | 64.2 ± 7.8 | 64.2 ± 9.5 | 68.2 ± 5.6 | 63.9 ± 5.1 |
| **Age at death, y** | — | 67.9 ± 7.5 | 66.9 ± 9.3 | 71.6 ± 5.9 | 67.7 ± 4.4 |
| **Sex, M/F** | 8/5 | 15/14 | 8/6 | 2/3 | 5/5 |
| **Education, y** | 17.1 ± 3.2 | 14.8 ± 2.9 | 14.0 ± 2.7 | 15.2 ± 1.1 | 15.0 ± 2.9 |
| **MDRS-2 total score** | — | 103.6 ± 23.4 | 105.0 ± 26.2 | 111.0 ± 10.4 | 98.5 ± 28.6 |
| **TOLA sum of standard scores** | — | 25.3 ± 7.0 | 24.5 ± 2.7 | 25.3 ± 5.2 | 26.5 ± 4.7 |
| **WAIS-III vocabulary score** | — | 41.3 ± 14.2 | 43.3 ± 12.2 | 40.2 ± 11.0 | 39.2 ± 10.5 |
| **Side of more severely involved limbs, R/L** | — | 12/17 | 6/8 | 2/3 | 5/5 |
| **Finger tapping, number of taps, dominant hand** | — | 25.5 ± 14.2 | 26.1 ± 21.9 | 25.1 ± 14.9 | 25.6 ± 5.8 |
| **Finger tapping, number of taps, nondominant hand** | — | 21.9 ± 9.2 | 19.6 ± 7.6 | 21.6 ± 9.5 | 25.4 ± 8.1 |

Abbreviations: AD = Alzheimer disease; CBD = corticobasal degeneration; HC = healthy control; MDRS-2 = Mattis Dementia Rating Scale–2; PSP = progressive supranuclear palsy; TOLA = Test of Oral and Limb Apraxia; WAIS-III = Wechsler Adult Intelligence Scale III.
Data reported as mean ± SD.

to protocols published previously.[14] Neuropathologic diagnoses were made using published criteria.[15–21] Neuropathologic diagnoses at the single-subject level are described in table 2. The primary pathologic diagnosis was used to divide the patients with CBS into the following subgroups: CBS-CBD, CBS-AD, and CBS-PSP.

## Healthy controls (HCs)

Thirteen HC participants matched on demographics were selected to undergo the same procedures at the NIH Clinical Center (table 1). All participants were evaluated by a board-certified neurologist and found neurologically normal. None of the HC participants presented with any cognitive or motor complaint and all presented with an unremarkable medical history.

## Standard protocol approvals, registrations, and patient consents

All patients gave written assent for the study. The study and consent procedure were approved by the NINDS institutional review board and by the Indiana University institutional review board. Sample and data storage and analysis including de-identification were compliant with Health Insurance Portability and Accountability Act (HIPAA) rules and the Declaration of Helsinki. HCs were compensated for their participation in the study.

## FDG-PET acquisition and analysis

Participants fasted after midnight on the day of their scan and had no caffeine, alcohol, or nicotine for 24 hours before the scan. During the 25 minutes after FDG injection, patients rested with their eyes covered and ears plugged and were instructed to remain awake. The patients underwent FDG-PET scans on a GE (Cleveland, OH) Advance scanner (4.25-mm slice separation, 35 slices, axial field of view 15.3 cm, transverse field of view 55.0 cm). Forty-five minutes after injection, a 2-minute positioning scan was performed, and then a 10-minute emission scan immediately followed by an 8-minute transmission scan (used to correct the emission data for attenuation) were obtained. Acquisition was performed in 3D mode. Images were reconstructed using an ordered subset-expectation maximization algorithm. Images were then exported as DICOM files and transformed to analyze files for subsequent postprocessing.

To account for the usually asymmetric nature of CBS, scans were flipped in order to represent the hemisphere contralateral to the most affected limbs on the right side of the image.[22] FDG-PET images were subjected to affine and nonlinear spatial normalization into Talairach and Tournoux space using SPM12 (Wellcome Department of Cognitive Neurology, London, UK). All the default choices of statistical parametric mapping (SPM) were followed with the exception of spatial normalization. For this study, the $^{15}H_2O$ SPM-default template was replaced by a dementia-optimized brain FDG-PET template as described by Della Rosa et al.[23] The spatially normalized set of images was then smoothed with a 10-mm isotropic Gaussian filter to blur individual variations in gyral anatomy and to increase the signal-to-noise ratio. In addition, a conjunction analysis was used to identify common clusters of hypometabolism among neuropathologic subgroups. This approach tests for the conjunction of different hypotheses (each specified by a contrast) by assessing the significance of the contrasts combined and then eliminating voxels that evidenced significant differences (i.e., interactions) among the different

**Table 2** Main neuropathologic diagnoses and coexisting pathologic findings at the individual patient level

| Clinical diagnosis | Main pathologic diagnosis | Coexisting pathologic findings |
|---|---|---|
| **CBS** | AD | CVD |
| **CBS** | AD | CVD |
| **CBS** | AD | CVD |
| **CBS** | AD | CVD |
| **CBS** | AD | CVD |
| **CBS** | AD | Lewy body disease |
| **CBS** | AD | Lewy body disease |
| **CBS** | AD | Lewy body disease |
| **CBS** | AD | Lewy body disease |
| **CBS** | AD | Lewy body disease |
| **CBS** | CBD | AD |
| **CBS** | CBD | AD |
| **CBS** | CBD | Lewy body disease |
| **CBS** | CBD | CVD |
| **CBS** | CBD | CVD |
| **CBS** | CBD | CVD |
| **CBS** | CBD | CVD |
| **CBS** | CBD | CVD |
| **CBS** | CBD | CVD |
| **CBS** | CBD | CVD |
| **CBS** | CBD | CVD |
| **CBS** | CBD | CVD |
| **CBS** | CBD | CVD |
| **CBS** | CBD | CVD |
| **CBS** | PSP | AD |
| **CBS** | PSP | AD |
| **CBS** | PSP | CVD |
| **CBS** | PSP | CVD |
| **CBS** | PSP | CVD |

Abbreviations: AD = Alzheimer disease; CBS = corticobasal syndrome; CBD = corticobasal degeneration; CVD = cerebrovascular disease; PSP = progressive supranuclear palsy.

contrasts,[24] thus allowing, in our case, the highlighting of areas that are hypometabolic compared to controls irrespective of the underlying pathology. A threshold of $p < 0.05$ (voxel-level) family-wise error (FWE)–corrected for multiple comparisons and a minimum cluster size of 100 was applied to all analyses except for the comparison between patients with CBS-PSP and controls where, given the low number of patients in the CBS-PSP group, a threshold of uncorrected $p < 0.0001$ was used, and for the correlations with clinical scores, where a threshold of uncorrected $p < 0.001$ was used. Age at the time of the PET scan and sex were used as nuisance variables.

Finally, to visually describe the pattern of hypometabolism at the single-subject level and thus to aid in the interpretation of the group analyses, we selected the following regions based on published studies[25–27]: FDG-PET patterns and neuropathologic data for AD, PSP, and CBD, i.e., anterior and posterior cingulate (both as separate values and as an anterior–posterior asymmetry index), precuneus, striatum (limited to the neostriatum, i.e., putamen and caudate nuclei), and midbrain. Regions of interest (ROI) were defined using the Automated Anatomical Labeling atlas and to account for asymmetry, we selected the lower value between the left and right hemisphere mask for each ROI. All data are calculated after whole brain normalization and reported as $z$ scores based on HC data. Given the focus on group analyses and the descriptive nature of this work, ROI data are reported only using median and range of observed values.

### Data availability statement

Anonymized data will be made available to qualified investigators for collaborative research in accordance with HIPPA guidelines.

## Results

### Clinical features and pathologic examinations

The primary pathologic diagnoses of enrolled patients after the neuropathologic examination were as follows: CBD (14 patients), AD (10 patients), and PSP (5 patients). Groups were matched on education and time between FDG-PET and death (overall effect education: $p = 0.55$, time before death: $p = 0.28$) while CBS-AD patients were younger ($p = 0.002$). Clinical data are reported in table 1. There was no difference between the CBS groups in motor impairment as assessed with finger tapping (dominant hand $p = 0.91$; nondominant hand $p = 0.25$) and all patients presented with parkinsonism. There were no differences between groups in overall cognitive performance as assessed with the MDRS-2 (total score: $p = 0.20$), in apraxia as assessed with the TOLA ($p = 0.84$), or in language ability as assessed by WAIS-III Vocabulary subtest scores ($p = 0.45$).

### Pattern of hypometabolism in the whole CBS cohort compared to controls

Patients with CBS presented with markedly asymmetric frontoparietal hypometabolism, centered in the precentral and postcentral gyri (table 3 and figure 1). In the hemisphere contralateral to the more affected limbs, a large cluster of hypometabolism was found including the dorsolateral prefrontal gyri, the precentral and postcentral gyri, the insula, and more posteriorly the superior parietal lobule as well as a second cluster centered in the thalamus. In the hemisphere ipsilateral to the more affected limbs, a much smaller cluster was identified, with a hypometabolic focus in the precentral gyrus, extending to the superior and middle frontal gyri.

**Table 3** Localization of the significant cluster of hypometabolism compared to controls for the corticobasal syndrome (CBS) cohort as well as the CBS–corticobasal degeneration (CBS-CBD), CBS–Alzheimer disease (CBS-AD), and CBS–progressive supranuclear palsy (CBS-PSP) groups

| Cluster size | Peak *p*(FWE) | Peak T | Peak *p*(unc) | x, y, z (mm) | Hemisphere contralateral to the most affected limbs | | Hemisphere ipsilateral to the most affected limbs | |
|---|---|---|---|---|---|---|---|---|
| | | | | | Neuromorphometrics | AAL | Neuromorphometrics | AAL |
| **Regional hypometabolism compared to controls in the whole CBS cohort[a]** | | | | | | | | |
| **14,201** | 0.000 | 10.81 | $p < 0.001$ | 32, −10, 54 | Precentral gyrus, middle and superior frontal gyri | Superior, middle, and inferior frontal gyri; middle and posterior cingulum; precentral and postcentral gyri; angular gyrus; superior and inferior parietal lobule; insula | | |
| | 0.000 | 10.30 | $p < 0.001$ | 38, −14, 70 | Precentral and postcentral gyri | | | |
| | 0.000 | 9.85 | $p < 0.001$ | 58, 0, 46 | Precentral and postcentral gyri | | | |
| **680** | 0.000 | 7.39 | $p < 0.001$ | −30, −12, 72 | | | Precentral and superior frontal gyri | Precentral gyrus; superior and middle frontal gyrus |
| | 0.000 | 6.65 | $p < 0.001$ | −30, 6, 66 | | | Superior and middle frontal gyri | |
| **155** | 0.000 | 6.75 | $p < 0.001$ | 14, −16, 14 | Thalamus | Thalamus | | |
| **Regional hypometabolism compared to controls in the CBS-CBD cohort[a]** | | | | | | | | |
| **11,232** | 0.000 | 13.33 | $p < 0.001$ | 36, −16, 72 | Precentral and postcentral gyri | Superior, middle, and inferior frontal gyri; middle and posterior cingulum; precentral and postcentral gyri; angular gyrus; superior and inferior parietal lobule; insula; supramarginal gyrus | | |
| | 0.000 | 13.03 | $p < 0.001$ | 30, −14, 64 | Precentral gyrus; superior and middle frontal gyri | | | |
| | 0.000 | 11.33 | $p < 0.001$ | 6, 0, 34 | Middle cingulate gyrus | | | |
| **607** | 0.000 | 9.93 | $p < 0.001$ | 14, 6, 10 | Caudate | Thalamus; caudate | | |
| | 0.003 | 7.02 | $p < 0.001$ | 10, −12, 12 | Thalamus | | | |
| | 0.033 | 5.87 | $p < 0.001$ | 4, −8, −2 | Thalamus | | | |
| **195** | 0.000 | 8.38 | $p < 0.001$ | −12, 4, 10 | | | Caudate | Caudate |
| **292** | 0.001 | 7.78 | $p < 0.001$ | −26, −12, 74 | | | Precentral gyrus | Precentral gyrus; superior and middle frontal gyrus |
| | 0.026 | 5.98 | $p < 0.001$ | −30, 6, 66 | | | Superior frontal gyrus | |

Continued

**Table 3** Localization of the significant cluster of hypometabolism compared to controls for the corticobasal syndrome (CBS) cohort as well as the CBS–corticobasal degeneration (CBS-CBD), CBS–Alzheimer disease (CBS-AD), and CBS–progressive supranuclear palsy (CBS-PSP) groups *(continued)*

| Cluster size | Peak *p*(FWE) | Peak T | Peak *p*(unc) | x, y, z (mm) | Hemisphere contralateral to the most affected limbs | | Hemisphere ipsilateral to the most affected limbs | |
|---|---|---|---|---|---|---|---|---|
| | | | | | Neuromorphometrics | AAL | Neuromorphometrics | AAL |
| **Regional hypometabolism compared to controls in the CBS-AD cohort[a]** | | | | | | | | |
| **16,556** | 0.000 | 16.11 | $p < 0.001$ | 58, −64, −4 | Inferior temporal gyrus | Precentral and postcentral gyri; middle and posterior cingulate gyrus; superior parietal lobule; superior, middle and temporal gyrus; angular gyrus; precuneus; cuneus; occipital inferior gyrus | | |
| | 0.000 | 15.17 | $p < 0.001$ | 64, −52, 26 | Angular gyrus; supramarginal gyrus | | | |
| | 0.000 | 14.67 | $p < 0.001$ | 56, −36, 36 | Supramarginal gyrus; parietal operculum | | | |
| **1,835** | 0.000 | 8.72 | $p < 0.001$ | −52, −34, 38 | | | Supramarginal gyrus | Supramarginal gyrus; superior parietal lobule |
| | 0.000 | 8.47 | $p < 0.001$ | −40, −44, 36 | | | Supramarginal gyrus | |
| | 0.001 | 8.13 | $p < 0.001$ | −64, −36, 20 | | | Supramarginal gyrus; superior temporal gyrus | |
| **1,805** | 0.001 | 8.17 | $p < 0.001$ | 30, −10, 60 | Precentral gyrus; superior frontal gyrus | Precentral gyrus; superior and middle frontal gyri | | |
| | 0.001 | 8.12 | $p < 0.001$ | 34, 8, 64 | Middle frontal gyrus | | | |
| | 0.001 | 8.08 | $p < 0.001$ | 18, −2, 74 | Superior frontal gyrus | | | |
| **840** | 0.001 | 8.00 | $p < 0.001$ | −20, −62, 68 | | | Superior parietal lobule | Precuneus; superior parietal lobule |
| | 0.024 | 6.21 | $p < 0.001$ | −30, −80, 50 | | | Angular gyrus | |
| **Regional hypometabolism compared to controls in the CBS-PSP cohort[b]** | | | | | | | | |
| **1,344** | 0.003 | 8.67 | $p < 0.001$ | 32, −10, 60 | Precentral gyrus; superior frontal gyrus | Precentral gyrus; superior and middle frontal gyrus | | |
| | 0.190 | 5.70 | $p < 0.001$ | 34, 4, 50 | Precentral and postcentral gyri | | | |
| | 0.338 | 5.28 | $p < 0.001$ | 56, −14, 58 | Middle frontal gyrus | | | |
| **688** | 0.079 | 6.30 | $p < 0.001$ | 60, 12, 14 | Precentral gyrus | Frontal inferior operculum; temporal pole; prefrontal gyrus | | |

Continued

**Table 3** Localization of the significant cluster of hypometabolism compared to controls for the corticobasal syndrome (CBS) cohort as well as the CBS–corticobasal degeneration (CBS-CBD), CBS–Alzheimer disease (CBS-AD), and CBS–progressive supranuclear palsy (CBS-PSP) groups *(continued)*

| Cluster size | Peak *p*(FWE) | Peak T | Peak *p*(unc) | x, y, z (mm) | Hemisphere contralateral to the most affected limbs | | Hemisphere ipsilateral to the most affected limbs | |
|---|---|---|---|---|---|---|---|---|
| | | | | | Neuromorphometrics | AAL | Neuromorphometrics | AAL |
| | 0.336 | 5.29 | $p < 0.001$ | 48, 8, 34 | Middle frontal gyrus | | | |
| **2,084** | 0.016 | 7.37 | $p < 0.001$ | 8, 18, 30 | Middle cingulate gyrus; anterior cingulate gyrus | Anterior and middle cingulate gyrus; supplementary motor area; superior medial frontal gyrus | | |
| | 0.092 | 6.20 | $p < 0.001$ | 6, −22, 30 | Middle cingulate gyrus | | | |
| | 0.098 | 6.16 | $p < 0.001$ | 10, 4, 52 | Supplementary motor cortex | | | |
| **173** | 0.039 | 6.78 | $p < 0.001$ | 16, 4, 12 | Caudate | Caudate | | |
| **102** | 0.200 | 5.67 | $p < 0.001$ | 56, 2, 46 | Precentral and postcentral gyri | Precentral gyrus | | |
| **Conjunction analysis among CBS-CBD, CBS-AD, and CBS-PSP[a]** | | | | | | | | |
| **447** | 0.000 | 7.52 | $p < 0.001$ | 32, −14, 68 | Precentral gyrus | Precentral gyrus; superior frontal gyrus | | |

Abbreviations: AAL = automatic anatomical labeling; FWE = family-wise error.
Patients vs control analyses are shown.
[a] Statistical significance set at $p < 0.05$ FWE-corrected for multiple comparisons, minimum cluster size: 100 voxels.
[b] Statistical significance set at $p < 0.0001$ uncorrected, minimum cluster size: 100 voxels.

**Figure 1** Regional hypometabolism compared to controls in the whole corticobasal syndrome cohort

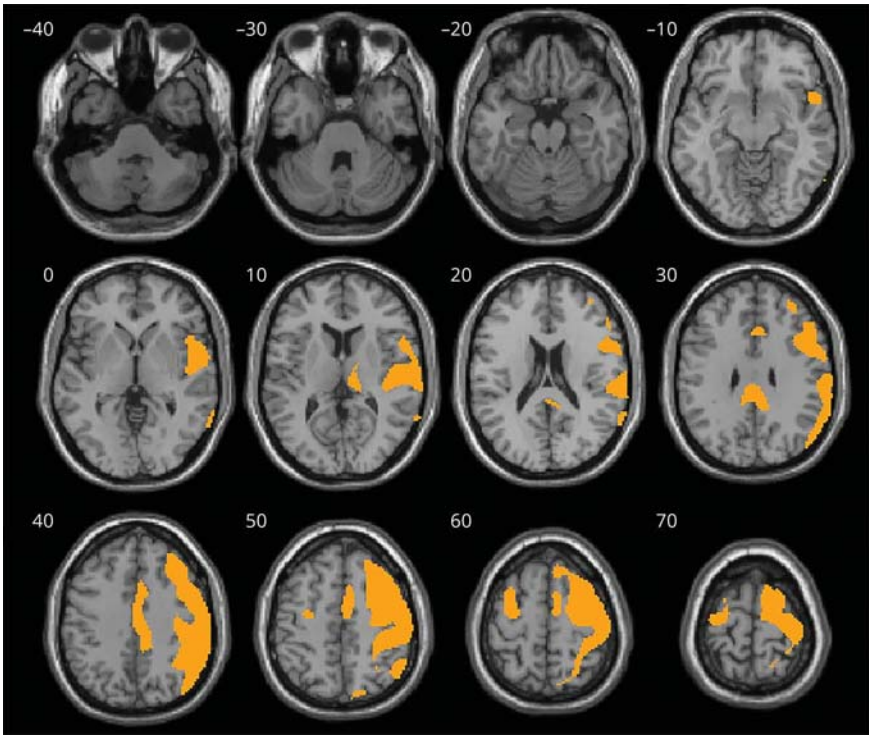


Statistical significance set at $p < 0.05$ family-wise error–corrected for multiple comparisons, minimum cluster size: 100 voxels. The right side of the image represents the hemisphere contralateral to the more severely affected limbs. Significant clusters overlaid on a volumetric brain MRI template.

## Pattern of hypometabolism correlations with clinical variables in the whole CBS cohort

In the whole CBS group, MDRS-2 performance directly correlated with metabolic levels in a frontal cluster including the superior and middle frontal gyri and the precentral gyrus located in the hemisphere contralateral to the more affected limbs (table 4 and figure 2A).

Finger tapping performance directly correlated with metabolic levels in bilateral fontal pole, anterior cingulate, basal ganglia, and orbitofrontal gyrus. Unilateral correlations were found in the insula and the ventral diencephalon, respectively, in the hemisphere contralateral and ipsilateral to the more affected limbs (table 4 and figure 2B).

Apraxia was directly associated with frontal hypometabolism in the superior and middle frontal gyri and in the supplementary motor cortex cluster, all in the hemisphere contralateral to the more affected limbs (table 4 and figure 2C).

Language deficits directly correlated with anterior insula and opercular metabolic levels in the hemisphere contralateral to the more affected limbs (table 4 and figure 2D).

## Pattern of hypometabolism in patients with CBS-CBD compared to controls

Patients with CBS-CBD presented with markedly asymmetric frontoparietal hypometabolism, centered in the precentral and postcentral gyri, and in the deep gray matter (table 3 and figure 3A). In the hemisphere contralateral to the more affected limbs, a large cluster of hypometabolism was found spanning from the superior, middle, and inferior frontal gyri, including the precentral and postcentral gyri, to the superior parietal lobule and the supramarginal gyrus, as well as a second hypometabolic cluster that included the thalamus and the caudate nucleus. In the hemisphere ipsilateral to the most affected limb, a much smaller cluster centered in the precentral gyrus and extending in the superior frontal gyrus was identified, together with caudate hypometabolism. There was no material change in results after removing CBS-CBD cases with a secondary pathologic diagnosis of coexisting AD or Lewy body disease (table 2). There was no significant difference in FDG-PET metabolism between CBS-CBD patients with and without concomitant AD pathology even at the lenient threshold of $p$(uncorrected) < 0.005.

## Pattern of hypometabolism in patients with CBS-AD compared to controls

Patients with CBS-AD presented with an asymmetric posterior hypometabolism, without deep gray matter involvement (table 3 and figure 3B). In the hemisphere contralateral to the most affected limbs, a large cluster of hypometabolism was found, including the inferior temporal gyrus and the angular gyrus, which extended to the posterior cingulate, the middle temporal gyri, and the superior parietal lobule. In the same hemisphere, a second, smaller cluster was also found, in

**Table 4** Localization of the significant cluster of hypometabolism correlated with clinical scores in the whole corticobasal syndrome (CBS) cohort

| Cluster size | Peak *p*(FWE) | Peak T | Peak *p*(unc) | x, y, z (mm) | Hemisphere contralateral to the most affected limbs | | Hemisphere ipsilateral to the most affected limbs | |
|---|---|---|---|---|---|---|---|---|
| | | | | | Neuromorphometrics | AAL | Neuromorphometrics | AAL |
| **Direct correlations between metabolism and MDRS-2 total score in the whole CBS cohort[a]** | | | | | | | | |
| **6,287** | 0.000 | 10.22 | $p < 0.001$ | 24, 6, 28 | Superior and middle frontal gyri | Superior, middle, and inferior frontal gyri; precentral and postcentral central gyrus; rolandic operculum | | |
| | 0.002 | 7.6 | $p < 0.001$ | 28, −2, 48 | Middle frontal gyrus; precentral gyrus | | | |
| **Direct correlations between metabolism and finger tapping total score in the whole CBS cohort[a]** | | | | | | | | |
| **7,253** | 0.004 | 6.91 | $p < 0.001$ | 0, 64, −2 | Superior frontal gyrus; frontal pole; superior frontal gyrus, medial segment | Superior frontal gyrus, medial segment; anterior cingulate; insula; putamen; pallidum | Superior frontal pole; superior frontal gyrus, medial segment | Superior frontal gyrus, medial segment; anterior cingulate; putamen; pallidum |
| **485** | 0.134 | 4.74 | $p < 0.001$ | −10, −22, −16 | | | Ventral diencephalon; brainstem | |
| **569** | 0.181 | 3.97 | $p < 0.001$ | 36, −6, −6 | Putamen, pallidum, posterior insula | Putamen, pallidum, insula | | |
| **Direct correlations between metabolism and TOLA: Sum of standard scores in the whole CBS cohort[a]** | | | | | | | | |
| **495** | 0.231 | 4.7 | $p < 0.001$ | 36, 6, 46 | Middle frontal gyrus; precentral gyrus | Precentral and postcentral gyri; middle frontal gyrus | | |
| **252** | 0.46 | 4.3 | $p < 0.001$ | 14, 6, 56 | Superior and middle frontal gyrus; supplementary motor cortex | Superior frontal gyrus; supplementary motor area | | |
| **Direct correlations between metabolism and WAIS-III vocabulary score in the whole CBS cohort[a]** | | | | | | | | |
| **324** | 0.251 | 4.5 | $p < 0.001$ | 32, −2, 24 | Anterior insula; central operculum; middle frontal gyrus; precentral gyrus | Insula; precentral gyrus; rolandic operculum; frontal inferior operculum | | |

Abbreviations: AAL = automatic anatomical labeling; FWE = family-wise error; MDRS-2 = Mattis Dementia Rating Scale–2; TOLA = Test of Oral and Limb Apraxia; WAIS-III = Wechsler Adult Intelligence Scale III.
Metabolism vs clinical scores analyses are shown.
[a] Statistical significance set at $p < 0.001$ uncorrected, minimum cluster size: 100 voxels.

the precentral gyrus. In the hemisphere ipsilateral to the most affected limbs, a smaller cluster was identified in the supramarginal gyrus, with a hypometabolic focus in the supramarginal gyrus and a smaller cluster in the superior parietal lobule. Of note, no cluster of hypometabolism was found in either the thalami or the basal ganglia in both hemispheres. There was no material change in results after taking out those CBS-AD cases with a secondary pathologic diagnosis of coexisting Lewy body disease (table 2). There was no significant difference in FDG-PET metabolism between patients with CBS-AD with and without concomitant Lewy body disease even at the lenient threshold of $p$(uncorrected) < 0.005.

## Pattern of hypometabolism in patients with CBS-PSP compared to controls

Patients with CBS-PSP presented with markedly asymmetric anterior hypometabolism (table 3 and figure 3C). In the hemisphere contralateral to the most affected limbs, the precentral gyrus, the middle and anterior cingulate gyri, the middle frontal gyri, and the caudate nucleus were hypometabolic. There were no foci of hypometabolism in the other hemisphere or in the midbrain. There was no significant difference in FDG-PET metabolism between patients with CBS-PSP with and without concomitant AD pathology even at the lenient threshold of $p$(uncorrected) < 0.005.

**Figure 2** Voxel-wise correlations

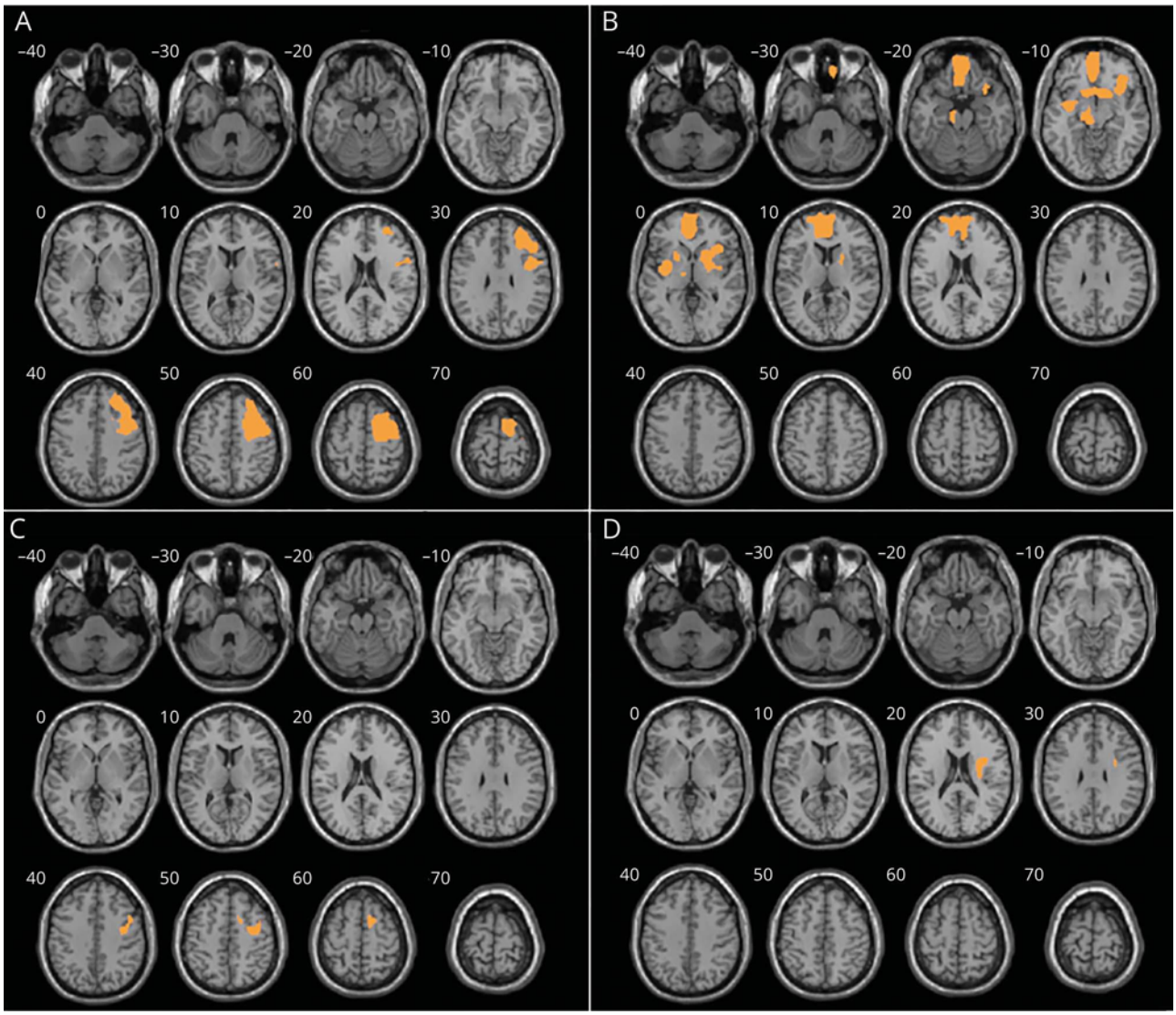


Voxel-wise correlations between $^{18}$Fluorodeoxyglucose–PET scans and Mattis Dementia Rating Scale–2 total score (A), finger tapping (B), Test of Oral and Limb Apraxia sum of standard scores (C), and Wechsler Adult Intelligence Scale III vocabulary score (D). Statistical significance set at $p < 0.001$ uncorrected for multiple comparisons, minimum cluster size: 100 voxels. The right side of the image represents the hemisphere contralateral to the more severely affected limbs. Significant clusters overlaid on a volumetric brain MRI template.

## Common areas of hypometabolism among the CBS-CBD, CBS-AD, and CBS-PSP groups

The conjunction analysis disclosed a cluster of hypometabolism focused in the precentral gyrus, extending in the superior frontal gyrus of the hemisphere contralateral to the most affected limbs, the only common area of hypometabolism among the CBS-CBD, CBS-AD, and CBS-PSP subgroups (table 3 and figure 3D). Visual inspection confirmed the presence of a reduction in FDG tracer retention in the precentral/postcentral gyrus region in all patients with CBS except 2 (included in the CBS-PSP and the CBS-AD groups).

## Patterns of hypermetabolism in the whole CBS cohort and the CBS-CBD, CBS-AD, and CBS-PSP groups compared to controls

There were no areas of relative hypermetabolism in the whole CBS cohort and the CBS-CBD, CBS-AD, and CBS-PSP groups compared to controls at the following thresholds: $p(\text{FWE}) < 0.05$, $p(\text{uncorrected}) < 0.005$.

## Regional hypometabolism differences at the single-subject level: Exploratory evidence

To further interpret the group results, median $z$ scores and the range of observed values are reported in table 5. There was a full separation of the observed values between CBS-AD and

**Figure 3** Regional hypometabolism

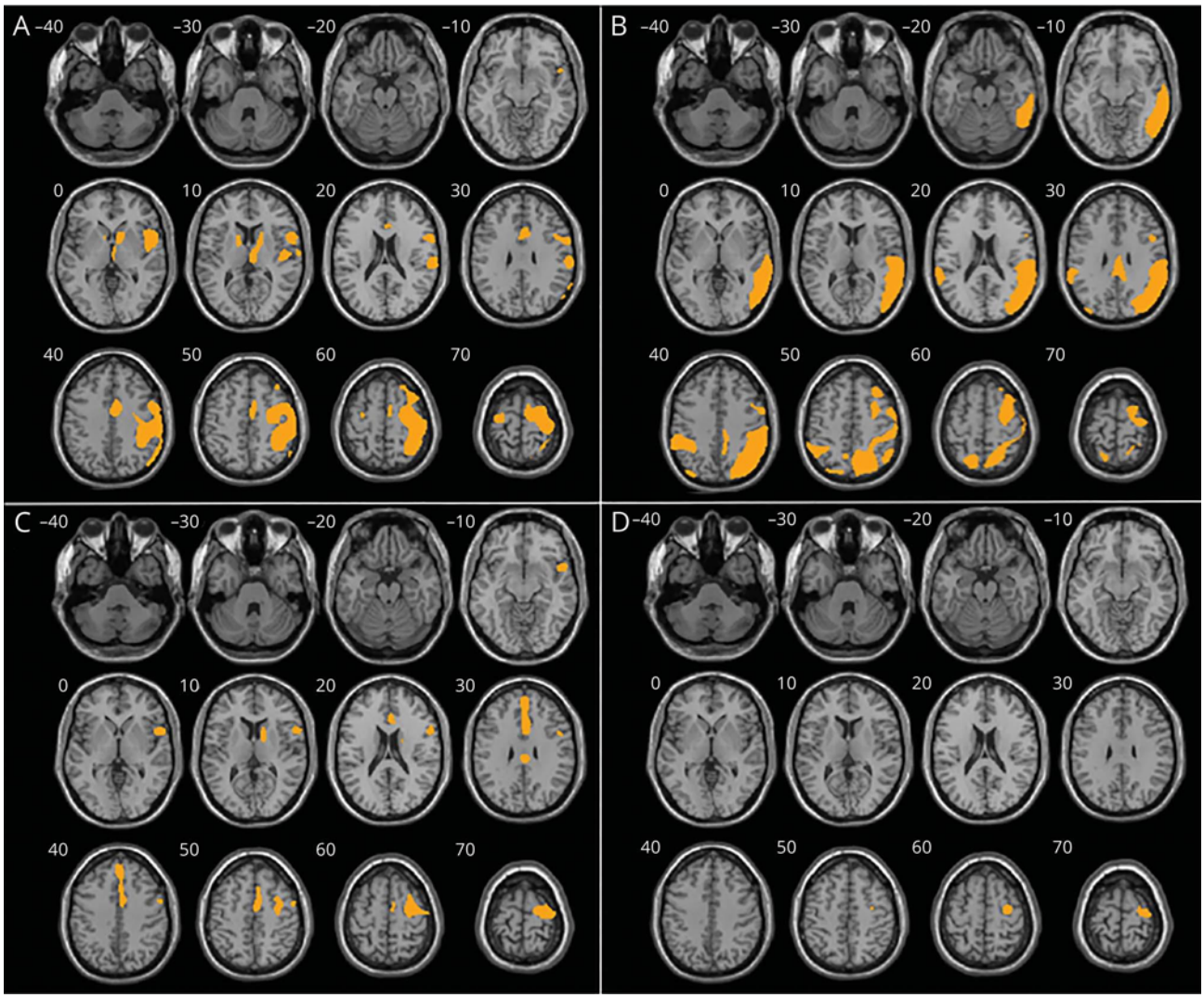


Regional hypometabolism compared to controls in the corticobasal syndrome (CBS)–corticobasal degeneration (CBD) (A), CBS–Alzheimer disease (B), and CBS–progressive supranuclear palsy (C) cohorts.(D) Conjunction analysis among the 3 groups. Statistical significance set at $p < 0.05$ family-wise error–corrected for multiple comparisons, except for C, where the threshold is $p < 0.0001$ uncorrected. Minimum cluster size: 100 voxels. The right side of the image represents the hemisphere contralateral to the more severely affected limbs. Significant clusters overlaid on a volumetric brain MRI template.

CBS-PSP in the following ROIs: anterior cingulate, precuneus, and the striatum, as well as on the anterior–posterior cingulate gradient. Moreover, there was a full separation between CBS-AD and CBS-CBD in the basal ganglia ROI and between CBS-PSP and CBS-CBD patients on the anterior–posterior cingulate asymmetry index.

## Discussion

We evaluated differences in topography of gray matter hypometabolism among different neuropathologic diagnoses underlying a CBS diagnosis, as assessed with FDG-PET. Our main findings at the group level were as follows: (1) overall a clinical diagnosis of CBS was associated with an asymmetric, large frontal, temporal, and parietal pattern of hypometabolism with a common hypometabolic cluster for all pathologic diagnoses in the precentral gyrus; and (2) the underlying pathology significantly modulated FDG uptake distribution, with typical posterior temporoparietal or medial–frontal patterns observed in patients with CBS with a pathologic diagnosis of AD or PSP, respectively, and frontoparietal cortex, thalamus, and caudate nucleus in CBS-CBD.

The hypometabolism pattern observed in the whole CBS group is consistent with previous reports of a marked asymmetric involvement of large cortical territories and of ipsilateral deep gray matter structures in this condition, which is thought to represent the metabolic footprint of the sensorymotor and cognitive expression of CBS,[6] as well as with the distribution of white matter abnormalities[28] and of gray matter atrophy described in this condition.[29] Published MRI

**Table 5** *z*Scores of FDG retention in selected regions of interest (ROIs), median (range)

| ROI *z* scores | CBS-AD | CBS-CBD | CBS-PSP |
|---|---|---|---|
| **Anterior cingulate** | 0.8 (−2.5 to 1.02) | −2.8 (−5.6 to 0.1) | −4.4 (−6.4 to −3.4) |
| **Posterior cingulate** | −3.77 (−6.0 to −0.6) | −2.4 (−5.4 to 0.8) | −0.8 (−1.6 to 0.8) |
| **Anterior–posterior cingulate gradient** | 3.7 (0.3 to 5.4) | −0.3 (−1.3 to 2.5) | −3.0 (−4.2 to −2.0) |
| **Precuneus** | −6.8 (−9.4 to −3.8) | −1.2 (−1.7 to 0.8) | −0.4 (−1.1 to 1.1) |
| **Striatum** | 0.5 (0.4 to 0.9) | −2.4 (−3.8 to −1.0) | −1.8 (−2.7 to −0.6) |
| **Midbrain** | 0.8 (−0.8 to 0.9) | 0.3 (−0.6 to 0.7) | 0.1 (−0.9 to 0.8) |

Abbreviations: AD = Alzheimer disease; CBD = corticobasal degeneration; CBS = corticobasal syndrome; FDG = $^{18}$Fluorodeoxyglucose; PSP = progressive supranuclear palsy.
Data reported as mean (range).

studied in CBS showed white matter damage in the perirolandic bundles and the body of the corpus callosum, i.e., those tracts connecting the primary and secondary sensory-motor cortices, which are the focus of cortical gray matter atrophy in this population.[28,29]

We observed that the primary pathology significantly affected the distribution of FDG-PET metabolism. A pathologic diagnosis of CBS-CBD was associated with an asymmetric hypometabolism involving the perisylvian frontotemporal cortex, the frontoparietal association cortex, the caudate nucleus, and the thalamus in the more affected hemisphere, as well as the caudate nucleus and the motor cortex in the less affected hemisphere. This pattern matches previous reports in a few cases of pathologically confirmed CBS-CBD[30] and it is in line with both tau imaging findings[31] and with the more common neuropathologic description of symptomatic CBD.[32]

Patients with CBS-AD presented with a posterior temporoparietal hypometabolic pattern, including large areas in association parietal cortex, the posterior cingulate cortex (PCC), and the precuneus (PC) in the more affected hemisphere but also a smaller cluster in parietal cortex in the less affected hemisphere. These regions are typically reported to be metabolically impaired in AD.[33,34] Hypometabolism in the PCC or the PC were not found in the CBS-CBD or the CBS-PSP subgroups. The findings in the CBS-AD group, moreover, confirm the observation of the posterior patterns of hypometabolism reported in patients with CBS presenting with positive in vivo biomarkers of amyloid deposition[9] and are in line with the more severe visuospatial impairment observed in patients with CBS-AD compared to patients with CBS without AD.[10] While a relative sparing of the deep gray structures is a common finding in AD and a feature that could help in the interpretation of FDG-PET scans,[35] moderate basal ganglia hypometabolism was observed in patients with CBS with positive in vivo markers of amyloid deposition.[9] That finding could also be due to the positivity of in vivo amyloid markers in non-AD conditions such as dementia with Lewy bodies,[36] which may show deep gray matter hypometabolism.[37] While more studies are needed to characterize the FDG-PET patterns in patients with CBS with positive amyloid imaging findings, these discrepancies also point to the caution needed in the interpretation of amyloid imaging to infer the underling pathology in patients with CBS.

Patients with CBS-PSP showed a focus of hypometabolism centered on the medial frontal gyrus, the anterior and middle cingulate gyri, and also involved the caudate nucleus in the more affected hemisphere. Again, the involvement of these structures was peculiar to this subgroup with the exception of the caudate nucleus (involved in CBS-CBD as well). This pattern has been reported in typical PSP, albeit in a more symmetric fashion.[38,39] In the literature, there are a few neuropathologic case series of CBS-PSP that showed a shift from subcortical nuclei to the middle frontal cortices as preferential sites of tau deposition, at least compared with patients with PSP with more classical presentations.[40,41] These data lend support to the cortical FDG-PET hypometabolism pattern observed in our CBS-PSP group compared to controls.

The availability of pathologic diagnoses, however, allowed us to evaluate not only the overall pattern of hypometabolism in our CBS population compared to controls, but also which regions were consistently hypometabolic across the neuropathologic diagnoses. In contrast with the relatively large region of hypometabolism in the whole CBS group, the precentral gyrus was the only area of FDG uptake reduction common to the CBS-CBD, CBS-AD, and CBS-PSP subgroups. This observation is in line with the key role played by motor processing dysfunction in CBS and with the perirolandic pattern of gray matter loss described in CBS.[29] Interestingly, in a functional MRI connectivity study performed in controls, this area has been shown to be the epicenter of a network composed of those areas more consistently involved in CBS,[42,43] i.e., to represent the region most strongly connected with the other components of the network.[42] From a clinical standpoint, the absence of this FDG-PET sign should challenge the diagnosis of CBS, irrespective of

the underlying pathologic substrate. FDG-PET hypometabolism in the precentral gyrus is not a common finding across neurodegenerative diseases, except in amyotrophic lateral sclerosis (ALS).[44] ALS, however, is not a common differential diagnosis in the CBS workup. If this finding is confirmed in an independent cohort, the presence of perirolandic FDG-PET hypometabolism should be evaluated in the workup of patients with CBS.

Taking into account the relative hypometabolism in selected regions based on the pattern observed at the group-level analysis, it was possible to observe a good separation among the 3 groups, especially between CBS-AD and the other 2 groups. This shows the consistency of the observed PET patterns also at the individual level. While the crux of this work was mainly focused on group comparisons, these results at the single-subject level are of interest and suggest that FDG-PET could be useful in the clinical setting to guide the identification of the pathology underlying CBS. The development of diagnostic markers at the single-subject level was not the aim of the study, also given the size of the sample. Future studies in independent populations are needed to confirm these findings at the single-subject level.

Our results do not imply that some clinical features could not be as useful as FDG-PET to help in the differentiation between pathologies underling CBS (indeed this was not the aim of our study). From a clinical point of view, our findings provide the description of FDG-PET patterns due to different pathologic substrata thus aiding in the interpretation of these images and in the characterization of the possible role of FDG-PET in CBS clinical care. Moreover, our observations support the hypothesis that different pathologic protein misfoldings tend to affect preferentially different regions of the brain[45,46] (i.e., that some brain regions are more prone, for example, to amyloid deposition, or 4-repeat tau deposition and so on) independently of the clinical phenotype. The biological bases of this regional vulnerability are to date poorly understood; however, they have been proposed to be linked to the difference in local gene expression. Recent evidence of this hypothesis has been provided by a recent study based on the Alzheimer's Disease Neuroimaging Initiative dataset and the Allen brain atlas of the adult human brain transcriptome showing that the regional expression of genes in the amyloid and tau cascade were respectively associated with amyloid PET and gray matter atrophy patterns.[47]

The finding of a common area of hypometabolism across the different groups (i.e., the precentral gyrus) is also relevant for the understanding of the mechanisms of neurodegeneration and support the hypothesis that network hub involvement (i.e., those regions densely connected with other areas) is a key factor in determining the clinical symptomatology irrespective of the cause of regional damage.[42]

Lack of tau-PET imaging scans (not available at the time of enrollment) and the years separating our imaging evaluation from the neuropathologic diagnosis prevented us from determining the association between local tau burden and FDG-PET metabolism. While more work is needed to shed light on this issue, some preliminary evidence is available in the literature showing a partial spatial overlap between FDG-PET and tau-PET patterns, albeit with a larger spatial extension of the latter.[48] Published evidence on tau-PET patterns in CBS points to a significant tracer retention in the perirolandic cortical areas and the basal ganglia similar to the FDG-PET findings reported in our cohort.[49]

We presented data on a relatively large number of patients with CBS with both FDG-PET and pathology data. Available FDG-PET cohort studies of CBS to date have lacked neuropathologic validation except for case reports or small series.[6] Using this combined FDG-PET and pathology approach, we were able to identify pathology-specific FDG-PET patterns of hypometabolism both at the group and at the single-subject level, which could be relevant for the day-to-day management of these difficult-to-treat patients, more so if proteinopathy-specific treatments become available. The main limitation of this study is the limited sample size of the pathologic subgroups due to the relative rarity of this condition, and the even rarer availability of FDG-PET and autopsy data from patients with CBS. As expected from the neurodegenerative conditions literature,[50] some patients present with a primary pathologic diagnosis of a neurodegenerative condition, but also demonstrate additional pathologic changes indicating the presence of other, relatively minor, coexisting pathologic processes. The results presented at the single-subject level, however, suggest that these additional neuropathologic processes do not significantly affect the main FDG-PET patterns observed.

Our study demonstrates that FDG-PET is an effective, complementary tool for proteinopathy identification in neurodegenerative diseases. Earlier identification of the underlying neurodegenerative disorder by PET in the coming era of expanded protein-specific radiopharmaceuticals imaging should permit faster and effective proteinopathy-specific treatments for our patients.

## Study funding

Supported by US Public Health Service P30AG10133 (B.G.) and the intramural program of the NIH/National Institute of Neurologic Disorders and Stroke.

## Disclosure

M. Pardini receives research support from Novartis and fees from Merck and Novartis. E. Huey, S. Spina, and W. Kreisl report no disclosures relevant to the manuscript. S. Morbelli receives speaker honoraria from GE Healthcare and Eli Lilly. E. Wassermann, F. Nobili, B. Ghetti, and J. Grafman report no disclosures relevant to the manuscript. Go to Neurology.org/N for full disclosures.

## Publication history

Received by *Neurology* June 3, 2018. Accepted in final form October 26, 2018.

## Appendix Authors

| Name | Location | Role | Contribution |
|---|---|---|---|
| **Matteo Pardini, MD, PhD** | University of Genoa, Italy | Author | Designed and conceptualized study, analyzed and interpreted the data, drafted the manuscript for intellectual content |
| **Edward D. Huey, MD, PhD** | Columbia University Medical Center, New York | Author | Designed and conceptualized study, analyzed and interpreted the data, drafted part of the manuscript, revised the manuscript for intellectual content |
| **Salvatore Spina, MD, PhD** | UCSF Memory and Aging Center, San Francisco, CA | Author | Analyzed and interpreted the data, drafted part of the manuscript, revised the manuscript for intellectual content |
| **William C. Kreisl, MD, PhD** | Columbia University Medical Center, New York | Author | Analyzed and interpreted the data, drafted part of the manuscript, revised the manuscript for intellectual content |
| **Silvia Morbelli, MD, PhD** | University of Genoa, Italy | Author | Analyzed and interpreted the data, drafted part of the manuscript, revised the manuscript for intellectual content |
| **Eric M. Wassermann, MD, PhD** | NIH, Bethesda, MD | Author | Analyzed and interpreted the data, drafted part of the manuscript, revised the manuscript for intellectual content |
| **Flavio Nobili, MD** | University of Genoa, Italy | Author | Analyzed and interpreted the data, drafted part of the manuscript, revised the manuscript for intellectual content |
| **Bernardino Ghetti, MD, PhD** | Indiana University School of Medicine, Indianapolis | Author | Designed and conceptualized study analyzed and interpreted the data, drafted part of the manuscript, revised the manuscript for intellectual content |
| **Jordan Grafman, PhD** | Shirley Ryan AbilityLab, Chicago, Illinois | Author | Designed and conceptualized study analyzed and interpreted the data, drafted part of the manuscript, revised the manuscript for intellectual content |

## References


1. Mathew R, Bak TH, Hodges JR. Diagnostic criteria for corticobasal syndrome: a comparative study. J Neurol Neurosurg Psychiatry 2012;83:405–410.
2. Boeve BF. The multiple phenotypes of corticobasal syndrome and corticobasal degeneration: implications for further study. J Mol Neurosci 2011;45:350–353.
3. Kouri N, Whitwell JL, Josephs KA, Rademakers R, Dickson DW. Corticobasal degeneration: a pathologically distinct 4R tauopathy. Nat Rev Neurol 2011;7:263–272.
4. Pellerin L, Magistretti PJ. Sweet sixteen for ANLS. J Cereb Blood Flow Metab 2012;32:1152–1166.
5. Eidelberg D, Dhawan V, Moeller JR, et al. The metabolic landscape of cortico-basal ganglionic degeneration: regional asymmetries studied with positron emission tomography. J Neurol Neurosurg Psychiatry 1991;54:856–862.
6. Niethammer M, Tang CC, Feigin A, et al. A disease-specific metabolic brain network associated with corticobasal degeneration. Brain 2014;137:3036–3046.
7. Taniwaki T, Yamada T, Yoshida T, et al. Heterogeneity of glucose metabolism in corticobasal degeneration. J Neurol Sci 1998;161:70–76.
8. Hammesfahr S, Antke C, Mamlins E, et al. FP-CIT and IBZM-SPECT in corticobasal syndrome: results from a clinical follow-up study. Neurodegener Dis 2016;16:342–347.
9. Sha SJ, Ghosh PM, Lee SE, et al. Predicting amyloid status in corticobasal syndrome using modified clinical criteria, magnetic resonance imaging and fluorodeoxyglucose positron emission tomography. Alzheimers Res Ther 2015;7:8.
10. Boyd CD, Tierney M, Wassermann EM, et al. Visuoperception test predicts pathologic diagnosis of Alzheimer disease in corticobasal syndrome. Neurology 2014;83:510–519.
11. Pardini M, Huey ED, Cavanagh AL, Grafman J. Olfactory function in corticobasal syndrome and frontotemporal dementia. Arch Neurol 2009;66:92–96.
12. Boeve BF, Lang AE, Litvan I. Corticobasal degeneration and its relationship to progressive supranuclear palsy and frontotemporal dementia. Ann Neurol 2003;54(suppl 5):S15–S19.
13. Huey ED, Pardini M, Cavanagh A, et al. Association of ideomotor apraxia with frontal gray matter volume loss in corticobasal syndrome. Arch Neurol 2009;66:1274–1280.
14. Spina S, Murrell JR, Huey ED, et al. Corticobasal syndrome associated with the A9D progranulin mutation. J Neuropathol Exp Neurol 2007;66:892–900.
15. Dickson DW, Bergeron C, Chin SS, et al. Office of Rare Diseases neuropathologic criteria for corticobasal degeneration. J Neuropathol Exp Neurol 2002;61:935–946.
16. Litvan I, Hauw JJ, Bartko JJ, et al. Validity and reliability of the preliminary NINDS neuropathologic criteria for progressive supranuclear palsy and related disorders. J Neuropathol Exp Neurol 1996;55:97–105.
17. Dickson DW, Lin W, Liu WK, Yen SH. Multiple system atrophy: a sporadic synucleinopathy. Brain Pathol 1999;9:721–732.
18. Knopman DS, Mastri AR, Frey WH, II, Sung JH, Rustan T. Dementia lacking distinctive histologic features: a common non-Alzheimer degenerative dementia. Neurology 1990;40:251–256.
19. The Lund and Manchester Groups. Clinical and neuropathological criteria for frontotemporal dementia.J Neurol Neurosurg Psychiatry 1994;57:416–418.
20. Hyman BT, Phelps CH, Beach TG, et al. National Institute on Aging–Alzheimer's Association guidelines for the neuropathologic assessment of Alzheimer's disease. Alzheimers Dement 2012;8:1–13.
21. Mackenzie IR, Neumann M, Bigio EH, et al. Nomenclature and nosology for neuropathologic subtypes of frontotemporal lobar degeneration: an update. Acta Neuropathol 2010;119:1–4.
22. Whitwell JL, Jack CR, Jr., Boeve BF, et al. Imaging correlates of pathology in corticobasal syndrome. Neurology 2010;75:1879–1887.
23. Della Rosa PA, Cerami C, Gallivanone F, et al. A standardized [18F]-FDG-PET template for spatial normalization in statistical parametric mapping of dementia. Neuroinformatics 2014;12:575–593.
24. Price CJ, Friston KJ. Cognitive conjunction: a new approach to brain activation experiments. Neuroimage 1997;5:261–270.
25. Nestor PJ, Altomare D, Festari C, et al. Clinical utility of FDG-PET for the differential diagnosis among the main forms of dementia. Eur J Nucl Med Mol Imaging 2018;45:1509–1525.
26. Teune LK, Bartels AL, de Jong BM, et al. Typical cerebral metabolic patterns in neurodegenerative brain diseases. Mov Disord 2010;25:2395–2404.
27. Kouri N, Murray ME, Hassan A, et al. Neuropathological features of corticobasal degeneration presenting as corticobasal syndrome or Richardson syndrome. Brain 2011;134:3264–3275.
28. Tovar-Moll F, de Oliveira-Souza R, Bramati IE, et al. White matter tract damage in the behavioral variant of frontotemporal and corticobasal dementia syndromes. PLoS One 2014;9:e102656.
29. Lee SE, Rabinovici GD, Mayo MC, et al. Clinicopathological correlations in corticobasal degeneration. Ann Neurol 2011;70:327–340.
30. Josephs KA, Whitwell JL, Tacik P, et al. [18F]AV-1451 tau-PET uptake does correlate with quantitatively measured 4R-tau burden in autopsy-confirmed corticobasal degeneration. Acta Neuropathol 2016;132:931–933.
31. Perani D, Cerami C, Caminiti SP, et al. Cross-validation of biomarkers for the early differential diagnosis and prognosis of dementia in a clinical setting. Eur J Nucl Med Mol Imaging 2016;43:499–508.
32. Ling H, Kovacs GG, Vonsattel JP, et al. Astrogliopathy predominates the earliest stage of corticobasal degeneration pathology. Brain 2016;139:3237–3252.
33. Bohnen NI, Djang DS, Herholz K, Anzai Y, Minoshima S. Effectiveness and safety of 18F-FDG PET in the evaluation of dementia: a review of the recent literature. J Nucl Med 2012;53:59–71.
34. Marcus C, Mena E, Subramaniam RM. Brain PET in the diagnosis of Alzheimer's disease. Clin Nucl Med 2014;39:e413–422; quiz e423–e426.
35. Herholz K, Carter SF, Jones M. Positron emission tomography imaging in dementia. Br J Radiol 2007;80 Spec No 2:S160–S167.
36. Gomperts SN, Rentz DM, Moran E, et al. Imaging amyloid deposition in Lewy body diseases. Neurology 2008;71:903–910.

37. Miyazawa N, Shinohara T, Nagasaka T, Hayashi M. Hypermetabolism in patients with dementia with Lewy bodies. Clin Nucl Med 2010;35:490–493.
38. Eckert T, Barnes A, Dhawan V, et al. FDG PET in the differential diagnosis of parkinsonian disorders. Neuroimage 2005;26:912–921.
39. Niccolini F, Politis M. A systematic review of lessons learned from PET molecular imaging research in atypical parkinsonism. Eur J Nucl Med Mol Imaging 2016;43: 2244–2254.
40. Tsuboi Y, Josephs KA, Boeve BF, et al. Increased tau burden in the cortices of progressive supranuclear palsy presenting with corticobasal syndrome. Mov Disord 2005;20:982–988.
41. Ling H, de Silva R, Massey LA, et al. Characteristics of progressive supranuclear palsy presenting with corticobasal syndrome: a cortical variant. Neuropathol Appl Neurobiol 2014;40:149–163.
42. Zhou J, Gennatas ED, Kramer JH, Miller BL, Seeley WW. Predicting regional neurodegeneration from the healthy brain functional connectome. Neuron 2012;73: 1216–1227.
43. Seeley WW, Crawford RK, Zhou J, Miller BL, Greicius MD. Neurodegenerative diseases target large-scale human brain networks. Neuron 2009;62:42–52.
44. Agosta F, Altomare D, Festari C, et al. Clinical utility of FDG-PET in amyotrophic lateral sclerosis and Huntington's disease. Eur J Nucl Med Mol Imaging 2018;45:1546–1556.
45. Whitwell JL, Jack CR, Jr., Przybelski SA, et al. Temporoparietal atrophy: a marker of AD pathology independent of clinical diagnosis. Neurobiol Aging 2011;32: 1531–1541.
46. Warren JD, Rohrer JD, Schott JM, Fox NC, Hardy J, Rossor MN. Molecular nexopathies: a new paradigm of neurodegenerative disease. Trends Neurosci 2013;36:561–569.
47. Grothe MJ, Sepulcre J, Gonzalez-Escamilla G, et al. Molecular properties underlying regional vulnerability to Alzheimer's disease pathology. Brain 2018;141:2755–2771.
48. Ossenkoppele R, Schonhaut DR, Scholl M, et al. Tau PET patterns mirror clinical and neuroanatomical variability in Alzheimer's disease. Brain 2016;139:1551–1567.
49. Kikuchi A, Okamura N, Hasegawa T, et al. In vivo visualization of tau deposits in corticobasal syndrome by 18F-THK5351 PET. Neurology 2016;87:2309–2316.
50. Boyle PA, Yu L, Wilson RS, Leurgans SE, Schneider JA, Bennett DA. Person-specific contribution of neuropathologies to cognitive loss in old age. Ann Neurol 2017;83: 74–83.

# FDG-PET patterns associated with underlying pathology in corticobasal syndrome

Matteo Pardini, Edward D. Huey, Salvatore Spina, et al.

*Neurology* 2019;92;e1121-e1135 Published Online before print January 30, 2019
DOI 10.1212/WNL.0000000000007038